Interband, collective and atomic (p, d) excitations from 2 to 160 eV in Sc, Y, lanthanides and actinides and in some of their compounds by FEELS

M. Cukier, B. Gauthe, C. Wehenkel

Classification
Physics Abstracts
32.80 — 78.40 — 78.20D — 79.20K

Interband, collective and atomic (p, d) excitations from 2 to 160 eV in Sc, Y, lanthanides and actinides and in some of their compounds by FEELS

M. Cukier, B. Gauthe and C. Wehenkel

Spectroscopie Atomique et Ionique (*), Bâtiment 350, 91405 Orsay, France.

(*Reçu le 14 décembre 1979, accepté le 18 mars 1980*)

Résumé. — L'analyse des spectres de pertes d'énergie des électrons rapides a permis de déterminer dans un domaine d'énergie étendu les diverses constantes optiques des métaux et composés suivants : Sc, Sc_2O_3, Y, Y_2O_3, Gd, Gd_2O_3, Dy, LaF_3, GdF_3, DyF_3, Th, ThF_4, U et UF_4. Pour la première fois, une étude d'ensemble des spectres 3p à 6p a été effectuée entre 30 et 60 eV, Z variant de 21 à 92. Des analogies entre ces différents spectres p sont mises en évidence et discutées à la lumière de travaux théoriques récents. En dessous de 30 eV, des transitions inter-bandes intenses sont observées dans les isolants (sesquioxydes et fluorures), alors que les spectres des métaux sont dominés par des excitations collectives. A plus haute énergie, les spectres 4d des lanthanides et les spectres 5d des actinides sont comparés aux mesures de photoabsorption dans le domaine X-UV.

Abstract. — Fast electron energy loss spectroscopy (FEELS) is used to obtain the various optical constants over a large energy range in Sc, Sc_2O_3, Y, Y_2O_3, Gd, Gd_2O_3, Dy, LaF_3, GdF_3, DyF_3, Th, ThF_4, U and UF_4. For the first time a comprehensive study of the 3p to 6p spectra is performed in the 30-60 eV range, Z varying between 21 and 92. Interesting common features of these resonant p spectra are emphasized and discussed in the light of recent theoretical work. Below 30 eV, strong interband transitions are observed in the wide gap insulators (oxides and fluorides), while the metal spectra are dominated by collective or plasmon excitations. At higher energies, 4d-lanthanide and 5d-actinide spectra are compared with X-UV photoabsorption measurements.

1. **Introduction.** — A number of experimental studies has been devoted to the determination of optical properties of rare earth metals and of their oxides or fluorides [1-5] except in the 30-60 eV energy range including the 5p electron excitations where very few data are available. It seemed worthwhile to extend these studies over a larger energy scale and to attempt a comparison with actinides. However optical measurements in uranium and thorium and in their chemical compounds are still very scarce. The main purpose of this study is therefore to perform systematic comparisons over a wide energy range between photoabsorption cross-sections in metals situated at the beginning of the successive transition series in the periodic table and in some of their compounds. With this end in mind, we have derived the optical constants of these materials by a quantitative analysis of electron energy loss spectra investigated with the same experimental method from a few eV to 150 eV or more. Moreover the comparison between photoabsorption in the metal and in one of the corresponding compounds facilitates the separation of band structure effects from atomic excitations.

In addition, it was interesting in itself to investigate for the first time to our knowledge, the electron energy loss spectra in some fluorides.

2. **Experimental procedures.** — 2.1 SAMPLES PREPARATION. — The metal as well as fluoride foils were prepared in a high and clean vacuum (better than 10^{-7} torr) by fast evaporation of the bulk material. The films were deposited on glass plates at room temperature and their thicknesses measured by a quartz balance. In order to avoid any contact with water, the films were separated from their substrate by use of a thin collodion coating afterwards dissolved in an appropriate solvent; the samples were then lifted off and deposited without backing on tantalum specimen-holders or on fine copper mesh; all these operations were conducted in dry surroundings.

The sesquioxide samples (Sc_2O_3, Y_2O_3 and Gd_2O_3) have been obtained by heating (400 °C) self-supported metal films in a very pure oxygen flow; all of them displayed the typical diffraction pattern.

(*) ERA 719.

2.2 TESTING OF THE SAMPLE QUALITY. — Sc, Y and the rare earth metals are known as efficient getters of residual impurities when evaporated in vacuum devices. Obtaining a good sample quality requires therefore a high evaporation or deposition rate (more than 100 Å/s) and good clean vacuum ($\simeq 10^{-8}$ torr).

In order to obtain a more quantitative knowledge of the contamination effects or of the purity degree of our samples, we prepared a series of intentionally more or less contaminated Sc-layers (10 Å/s, 4×10^{-6} torr). The spectrum corresponding in figure 1 to pure scandium obtained with samples prepared in a 10^{-8} torr vacuum is used for the calculation of the optical constants in the later part of this paper. The same samples of pure, contaminated and oxidized scandium have been examined by P. Maletras and P. Vigier ([1]) using both fast electron diffraction and electron microscope techniques. The diffraction pattern of the oxidized sample corresponds to a pure c.c. structure, which proves the absence of unoxidized scandium in these layers.

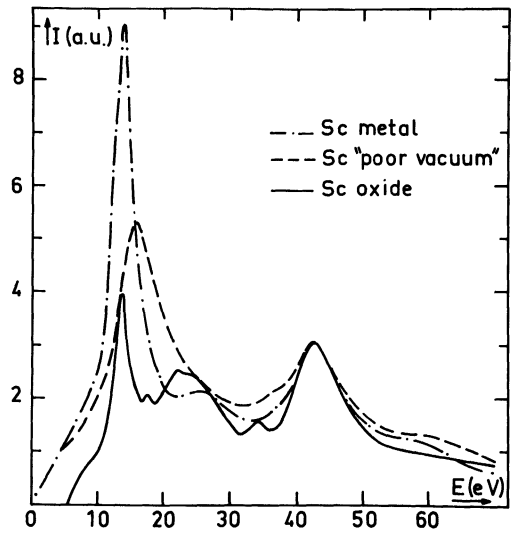

Fig. 1. — Experimental electron energy loss spectra in arbitrary units of scandium samples prepared in *poor vacuum* conditions (— — —) compared to those of pure metal (· — · — ·) and of its oxide (——) ; the shoulder on the Sc metal spectrum around 25 eV is due to double scattering.

In contrast, no difference can be observed between the diffraction patterns or the electron micrographs of the pure and contaminated scandium samples (Fig. 2) which both correspond to a pure h.c.p. structure. No trace of any f.c.c. hydride phase can be displayed in the diffraction pattern. These experimental facts allow some interesting conclusions :

i) The fast electron energy loss spectroscopy is a very sensitive tool for the detection of amorphous

([1]) Laboratoire de Microscopie Electronique, Université de Rouen, 76130 Mont St Aignan, France.

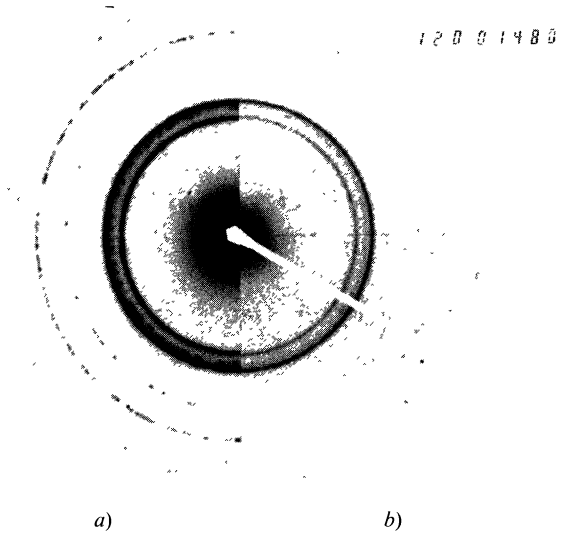

Fig. 2. — Typical h.c.p. diffraction patterns of pure (left part, *a*) and contaminated (right part, *b*) scandium samples.

contamination : in scandium the plasmon peak is shifted from 14 to 16 eV, the half-height width increases from about 4 to 11 eV, whereas its relative intensity decreases by a factor 2 ; the *smartness* of the main plasmon peak can therefore be considered as a good sample quality test.

ii) In contrast with previous work, no trace of scandium hydride can be detected in the contaminated samples : the contamination is certainly due to the carbon impurities present in classical vacuum devices.

iii) Good Sc, Y or rare earth samples must not be prepared by deposition on thin carbon layers because the exposure to the fast electron beam involves a solid state diffusion of the carbon atoms into the metal which leads to strongly distorted spectra in the lower energy range (see Fig. 3 in [16]).

2.3 APPARATUS. — The spectrometer is a Möllenstedt velocity analyser ; it uses a specially designed electrostatic lens [6] and collects electrons scattered by the samples over the 0 to 4 mrad. range. The energy resolution (full width at half maximum of the zero loss line) is better than 1 eV at a primary beam energy of 50 keV. A liquid nitrogen trap situated around the samples avoids the growth of a contamination layer under electron beam impact.

A surface barrier detector is connected to a 512 channel multiscale accumulating system (Zoomax SEIN) ; the whole spectrum is scanned in only 20 seconds with the dispersion usually employed (0.15 eV/channel) and so it is easy to repeat many times (100 or more) the exploration of a same spectrum and to improve the signal-to-noise ratio by accumulation. The spectra are continuously visualized on a screen so one can check that they remain

unaltered during accumulation. The spectra are then stored on magnetic tape in view of subsequent data processing.

3. **Spectra analysis and data processing.** — 3.1 THE PRINCIPLE OF THE METHOD. — The method developed by C. Wehenkel [7] is used to perform a self-consistent quantitative analysis of fast electron energy loss spectra; in this way the double (I_2) and triple (I_3) scattering contributions as well as surface losses (S) are calculated and substracted from experimental spectra (ES) in order to obtain the single scattering volume contribution (V). The knowledge of this volume contribution provides a means of determining the energy loss function Im $(-1/\varepsilon)$ where

$$\varepsilon = \varepsilon_1 + i\varepsilon_2$$

is the complex dielectric constant; Re $(1/\varepsilon)$ is then derived by a Kramers-Krönig analysis and the usual optical parameters like the normal reflectivity R, the linear photoabsorption coefficient μ or the photoabsorption cross-section σ are calculated from ε_1 and ε_2 values.

The effective number of electrons taking part in all excitations up to a given energy $\hbar\omega$ have also been computed by means of usual sum-rules [7]; it is often very useful, for the interpretation of our results, to compare these effective numbers calculated either for optical excitations $n_{\text{eff}}(\varepsilon_2)$ or for electron energy losses $n_{\text{eff}}(-\text{Im } 1/\varepsilon)$.

3.2 NORMALIZATION AND CHOICE OF ε FOR $\omega = 0$ IN INSULATING MATERIALS. — To perform the normalization of the energy loss function and the Kramers-Krönig analysis, it is necessary to use the dielectric constant value $\varepsilon(0)$ at $\hbar\omega = 0$. Whereas in metals Re $1/\varepsilon(0) = 0$ at $\omega = 0$, in dielectric materials like oxides or fluorides the $\varepsilon(0)$ value must be taken from published data. Only taking into account the electronic excitations and excluding other contributions to the dielectric constant at lower frequencies such as ionic polarization, we have taken $\varepsilon(0) = n^2$, where n is the refractive index in the visible or near infrared. These values of $\varepsilon(0)$ are reported in table I for each material investigated. They are appreciably lower than those used in some similar calculations previously carried out for oxides where the values of $\varepsilon(0)$ seem to originate from measurements in the radio-frequency range. As clearly shown in figure 3 in the case of the ThF_4 absorption curve, a too high

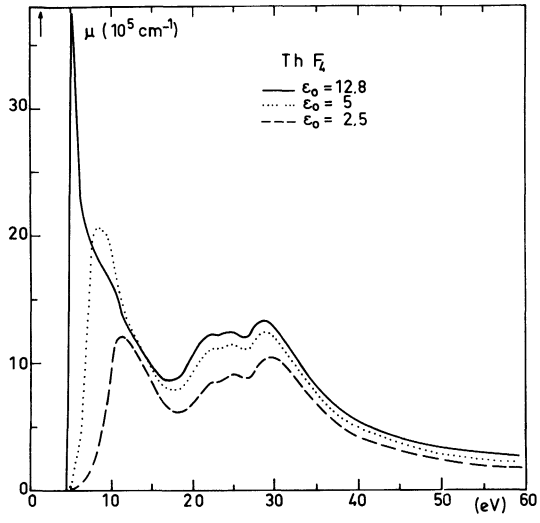

Fig. 3. — Photoabsorption coefficient of ThF_4 calculated from the same electron energy loss spectrum with three different values of $\varepsilon(0)$.

Table I. — *Values of* $\varepsilon(0)$ *used to normalize the optical constants.*

	Sc_2O_3	Y_2O_3	Gd_2O_3
ε_0	3.42	3.42	3.80
	LaF_3	GdF_3	DyF_3
ε_0	2.56	2.56	2.56
	ThF_4	UF_4	
ε_0	2.56	2.50	

Table II. — *Energy gap values estimated from experimental energy loss spectra.*

	Sc_2O_3	Y_2O_3	Gd_2O_3
gap	6 eV	5.4 eV	5 eV
	LaF_3	GdF_3	DyF_3
gap	6 eV	8 eV	8.6 eV
	ThF_4	UF_4	
gap	6 eV	6 eV	

value of $\varepsilon(0)$ gives rise to very steep and unrealistic variations of optical constants in the vicinity of the main absorption edge; in addition, such a choice of $\varepsilon(0)$ leads to an overestimate of all optical constants in the whole spectral range investigated.

3.3 ENERGY GAP VALUES IN INSULATORS. — The experimental energy loss spectra permits a direct determination of the energy gap values which are reported in table II.

4. **Results and discussion.** — 4.1 SCANDIUM, YTTRIUM, GADOLINIUM AND THEIR SESQUIOXIDES. — All these metals have the same external electron configuration (one d electron and two s electron) and open the successive transition metals series.

The volume loss spectra appear quite similar in all three metals and, as in Ti and V next to Sc in the first transition series [8, 9], display essentially below 50 eV two prominent peaks (Fig. 4), a narrow low energy peak around 13 eV followed, above 30 eV, by a broader and weaker peak.

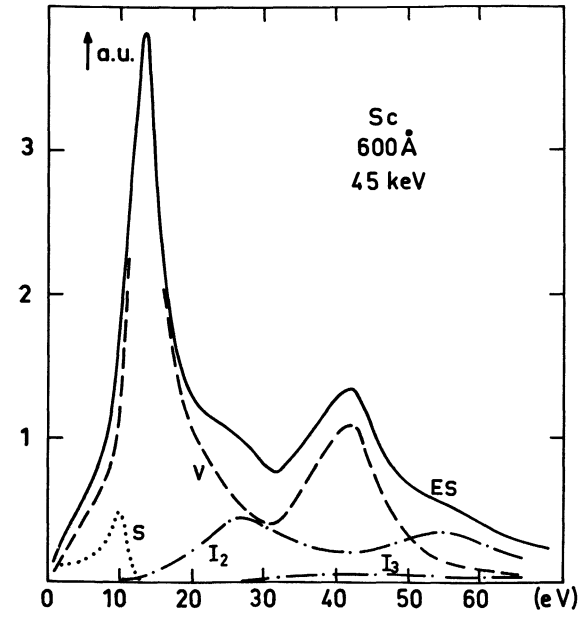

Fig. 4. — Analysis of the different contributions to the experimental energy loss spectrum (*ES*) of scandium : surface losses (*S*), volume single scattering (*V*), double scattering (I_2) and triple scattering (I_3).

4.1.1 *Scandium and* Sc_2O_3. — In scandium, the first volume-loss peak (Fig. 4), strong and relatively sharp, is situated at 13.5 eV in satisfactory agreement with the plasmon energy value (12.9 eV) calculated in the free electron model with all the three valence electrons taking part in the collective oscillations. This first peak, which is located in a region where ε_1 and ε_2 curves are almost structureless and of a right slope with $\varepsilon_1 \simeq 0$, $\varepsilon_2 \ll 1$, can therefore be clearly assigned to a volume plasmon excitation. It is also to be noted in this respect that the $n_{\text{eff}}(-\operatorname{Im} 1/\varepsilon)$ value calculated over the whole energy spread of this plasma peak actually reaches 3 around 30 eV. The collective origin of this first loss peak appears related to the fact discussed below that the onset of predominant interband transitions occurs in scandium beyond 30 eV, well above the plasmon value; the same situation is encountered in the next transition metal titanium [9].

The second prominent loss peak is associated with a broad absorption whose maximum is located around 38 eV (σ-curve, Fig. 5) and which is ascribed to the 3p electron excitation [10]; its onset is in reasonable agreement with the $M_{2,3}$ threshold value [11]. As in titanium and vanadium [8, 12], the absorption curve reaches its maximum appreciably beyond the $M_{2,3}$ threshold; this delayed maximum may be explained by atomic calculations [13, 14] which show most of the oscillator strength to be concentrated in transitions to the higher levels of $3p^5\ 3d^{n+1}$ configuration; a similar situation occurs in the 4d photoabsorption spectra of rare earths, as will be explained below.

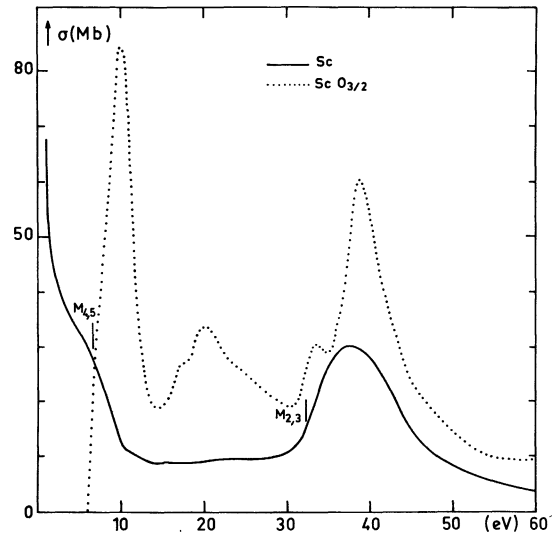

Fig. 5. — Derived photoabsorption cross-section of scandium (——) as compared to that of its oxide (.....); the vertical line indicates the $M_{2,3}$ energy level value reported in ref. [11].

The position of the 3p absorption peak in scandium confirms the regular increase of $M_{2,3}$ thresholds values with atomic number all along the first transition series [8, 12]. Going from scandium to its sesquioxide Sc_2O_3, the general shape of the volume loss spectrum is sensitively altered; although the oxide spectrum displays again two prominent peaks almost unchanged in position, some additional structures appear between them while the first main peak becomes much weaker (Fig. 1).

In Sc_2O_3 the σ-absorption curve derived from energy loss spectra rises steeply at the onset of interband transitions above an energy gap about 6 eV

wide (Fig. 5) and reaches a maximum around 10 eV; this sharp absorption peak is assigned to excitations from the filled O^- 2p valence band to the empty 3d-4s conduction band. However a higher energy part of these transitions is also probably responsible for the broad absorption peak located near 20 eV, as the 2p excitations are not yet exhausted at 30 eV, where $n_{eff}(\varepsilon_2) \simeq 7$ whereas the valence bonding band contains 9 electrons per half a molecule; actually all the electrons excited below 35 eV originate from the 2p valence band. A similar situation is encountered in lanthanide sesquioxides [15]. It is to be noted that the n_{eff} value calculated from the energy loss function reaches only 1.2 near 20 eV; it seems therefore somewhat arbitrary to associate the whole of the collective excitations exclusively with the first main peak located around 13.5 eV in the oxide energy loss spectrum. Due to the strong interband transitions described above, it appears more likely that the collective excitations are heavily modulated over an energy range extending up to about 35 eV by the 2p oscillator strength distribution.

At higher energy, the second prominent loss peak in Sc_2O_3 and the related absorption maximum are located at nearly the same position as in metallic scandium; they are also mostly associated with the excitation of the 3p electrons of the scandium ion [10]. This interpretation is in accordance with the $M_{2,3}$ energy level value as determined in scandium by photoemission measurements [11].

Concerning the energy loss values in scandium as in Sc_2O_3, our results are very close to those previously published [16, 17]. However the shapes and relative intensities of the prominent loss peaks are quite different, specially in metallic scandium where the low energy peak observed in the present work is much sharper and stronger.

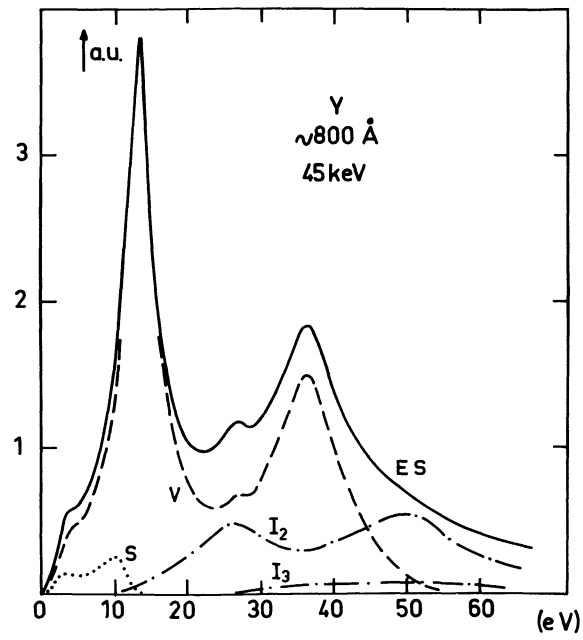

Fig. 6. — Analysis of the different contributions to the experimental energy loss spectrum (*ES*) of yttrium; the symbols have the same meaning as in figure 4.

4.1.2 *Yttrium, gadolinium and their sesquioxides.* — The electron energy loss spectra in these metals and oxides display again two prominent peaks (Figs. 6 and 7). In yttrium and gadolinium, the low energy loss of about 13 eV must be attributed to the excitation of a volume plasmon, along the lines already discussed for metallic scandium and in spite of a slight shift to higher energies as compared to the value calculated in a free electron model.

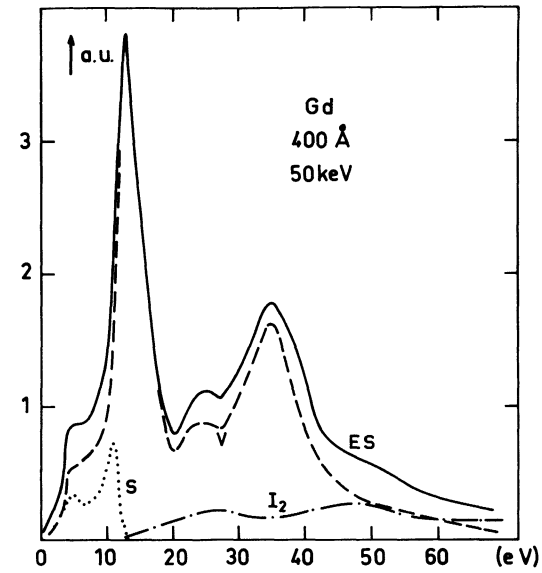

Fig. 7. — Analysis of the different contributions to the experimental energy loss spectrum (*ES*) of gadolinium; symbols as in figure 4.

In the sesquioxides Y_2O_3 and Gd_2O_3, the n_{eff} value derived from the energy loss function hardly reaches 1.5 around 20 eV and so it seems difficult to assign unambiguously the first main loss peak near 14.5 eV to a sharp plasma resonance. As in Sc_2O_3, the collective excitations appear strongly damped and modulated by individual transitions originating from the O^- 2p valence band and stretching over the same energy range. These interband transitions are responsible for the strong absorption peak rising steeply above 5 eV beyond the energy gap and which reaches a maximum near 10-12 eV (Figs. 8 and 9). In Y_2O_3 the ε_1 and ε_2 curves deduced from the present energy loss data are in satisfactory agreement with the results of independent optical measurements recently performed around the fundamental absorption edge [18].

The second major loss peak at a higher energy occurs around 36 eV in Y and 35 eV in Gd, at nearly the same position as in their sesquioxides : clearly it may be ascribed in both cases to the 4p (Y) and 5p (Gd) electron excitation. The corresponding absorption peak is located several eV beyond the $N_{2,3}$ or O_2 and O_3 energy level values (Figs. 8 and 9) as deter-

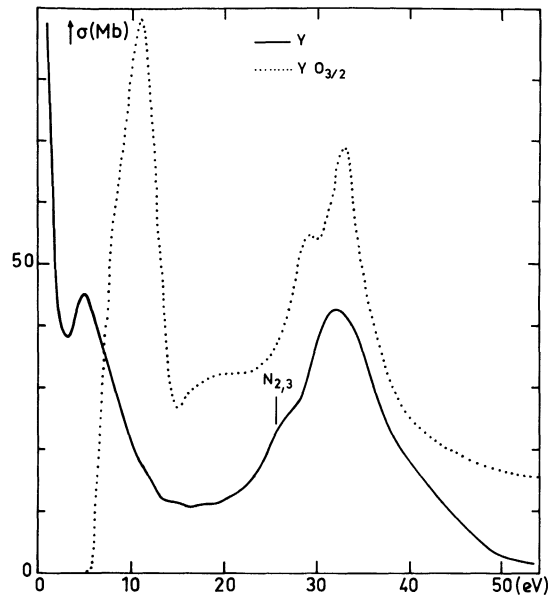

Fig. 8. — Derived photoabsorption cross-section of yttrium and of its oxide (.....) ; the vertical line indicates the $N_{2,3}$ energy level value reported in ref. [11].

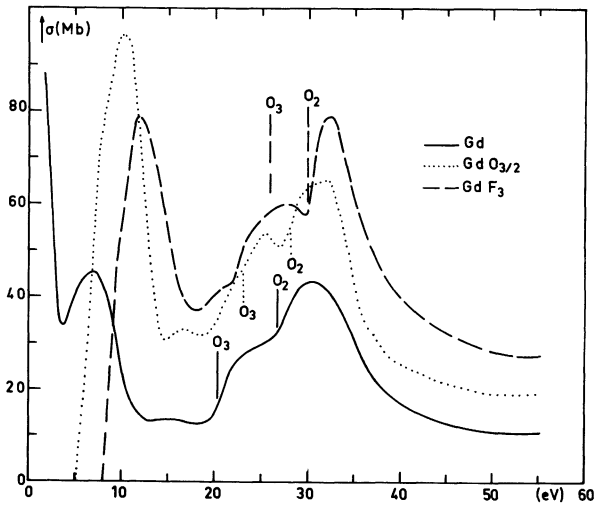

Fig. 9. — Derived photoabsorption cross-section of gadolinium, $GdO_{3/2}$ and GdF_3 ; the indicated O_2 and O_3 levels are given in ref. [19] for Gd and $GdO_{3/2}$ and in ref. [25] for GdF_3.

mined by photoemission experiments [11, 19]; as in Sc and Sc_2O_3, this resonant-like absorption peaking above the ionization threshold may be explained by atomic calculations [13, 14, 20, 21]. In addition and as expected, the energy value of this absorption maximum decreases regularly as going from Sc (38 eV) to Y (32 eV). The absorption curves in Gd and Gd_2O_3 display an additional shoulder on the low energy side of the second prominent peak (Fig. 9) which is probably related to the spin-orbit splitting of the initial $5p_{1/2}$-$5p_{3/2}$ states. However these spin-orbit doublets may be partly hidden in Gd_2O_3 by additional structure due to transitions from the valence band towards the upper part of the conduction band. A similar situation will be encountered in GdF_3 and DyF_3.

Our results are in approximate agreement with previously published data with regard to values of the major energy losses [15, 16, 22, 23]; nevertheless the spectra reported in this study look somewhat more structured and display stronger and sharper loss peaks. However the energy loss function derived in Y from optical measurements [24] exhibit a large peak around 5 eV which is not directly observed to our knowledge in the energy loss spectra so far reported.

The higher energy part of the Gd loss spectrum will be described below together with GdF_3 spectrum.

4.2 RARE EARTH TRIFLUORIDES. — As optical studies [3, 5] and photoemission measurements [25] have already been conducted on these fluorides, it was worthwhile to perform for the first time an analysis of fast electron energy loss spectra in some of these compounds and so to derive in an independent way their different optical properties. We have also investigated the Dy energy loss spectrum to attempt a comparison with its fluoride. The scanning of the spectra was extended towards higher energies (up to 140 eV in LaF_3 and 180 eV or more in GdF_3, Dy and DyF_3) in order to investigate the evolution of the 4d → 4f oscillator strengths with the number of vacancies available in the final subshell as compared with the case of the 3p excitation in the first series transition metals.

We shall distinguish two clearly separated regions : the low energy range (typically below 50 eV) and the region of 4d electron excitations above 100 eV.

4.2.1 *Low energy range.* — In all three fluorides investigated, the volume loss spectra show two prominent peaks of about the same magnitude (Figs. 10, 11, 12), unlike in the Gd and Dy spectra (Figs. 7

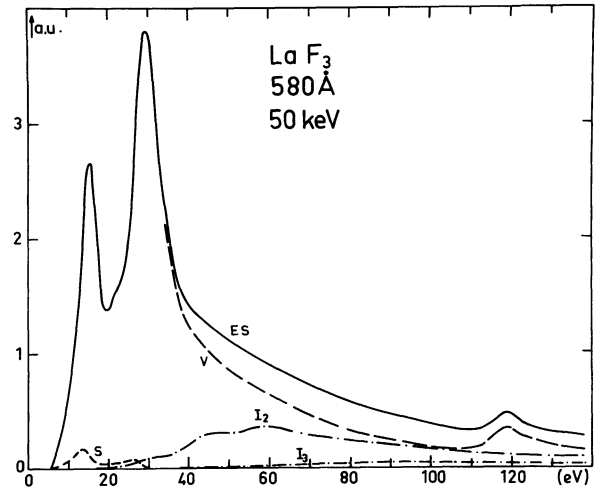

Fig. 10. — Analysis of the experimental energy loss spectrum of LaF_3 in its different contributions; symbols as in figure 4.

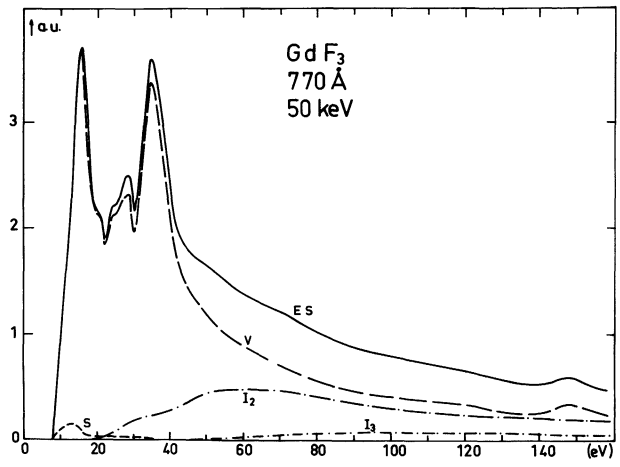

Fig. 11. — Analysis of the experimental energy loss spectrum of GdF_3 in its different contributions; symbols as in figure 4.

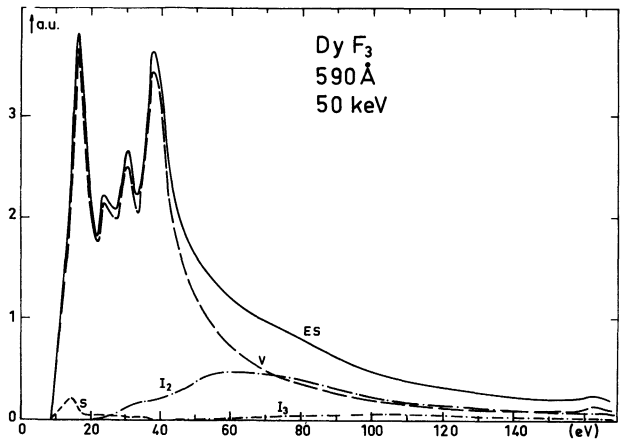

Fig. 12. — Analysis of the experimental energy loss spectrum of DyF_3 in its different contributions; symbols as in figure 4.

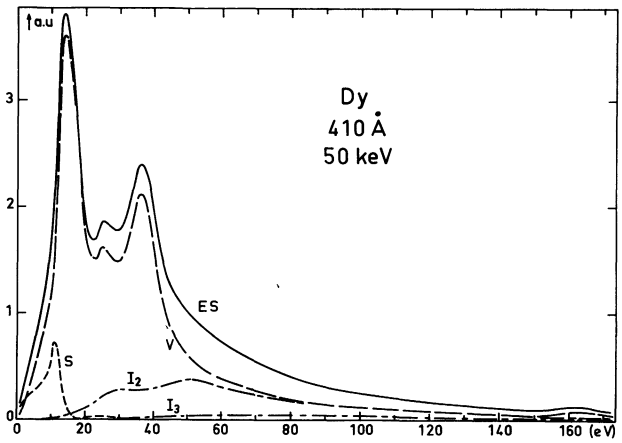

Fig. 13. — Analysis of the experimental energy loss spectrum of dysprosium.

and 13) where the first peak is considerably larger than the second one. Additional features located between the two main peaks in GdF_3 and DyF_3 spectra are much more structured than in the corresponding metal, with even one supplementary structure in DyF_3 as compared to Dy metal.

The derived photoabsorption curves (Figs. 14, 15, 9) show a first large peak located at about 12 eV in all these fluorides; this peak, also observed in reflectivity measurements [5], arises presumably from transitions between the filled F^- 2p valence band which contains 9 electrons per half a molecule and the empty lanthanide 5d-6s conduction band [5]. However the $n_{eff}(\varepsilon_2)$ values indicate that only about one third of the F^- 2p oscillator strength is exhausted at 20 eV and so the valence band excitations extend well beyond the onset of 5p electron excitations; as mentioned above a somewhat similar situation occurs in Sc_2O_3, Y_2O_3 and Gd_2O_3 for the O^- 2p valence band excitation.

Except in LaF_3, the next absorption peak exhibits some marked structure on its low energy side, parti-

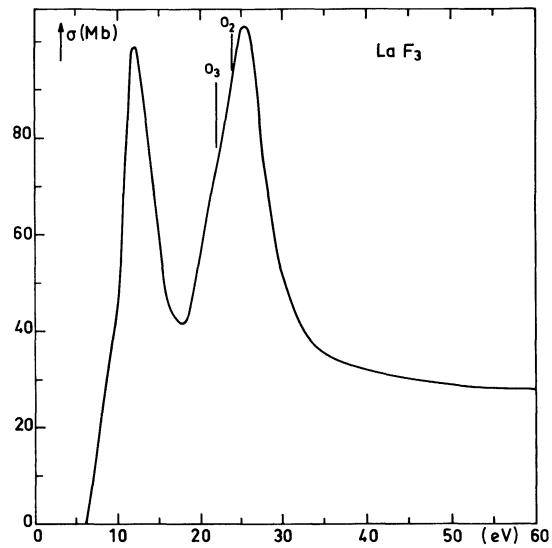

Fig. 14. — Derived photoabsorption cross-section of LaF_3; the positions of the O_2 and O_3 levels are reported from ref. [25].

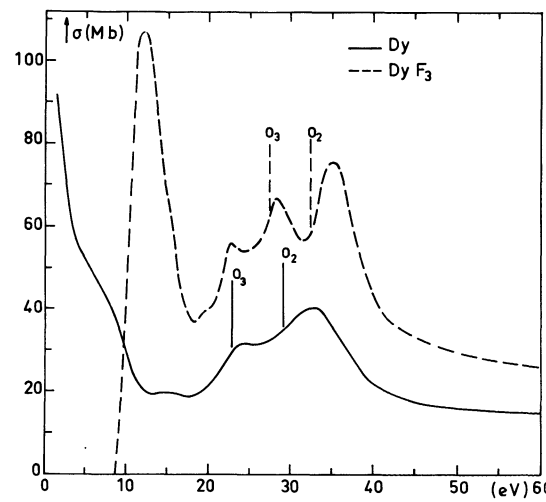

Fig. 15. — Derived photoabsorption cross-section of Dy and DyF_3; the O_2 and O_3 levels are reported from ref. [19] for Dy and from ref. [25] for DyF_3.

cularly in DyF_3 ; its onset is around 20 eV in each trifluoride whereas its maximum moves regularly to higher energies with increasing metal atomic number, varying from about 25 eV in LaF_3 to 32 eV in GdF_3 and 35 eV in DyF_3. The main part of this absorption peak is assigned to the lanthanide 5p electron excitation by comparison with X-ray photoemission data [25], which report in GdF_3 and DyF_3 a 5p levels spin-orbit splitting in reasonable agreement with the energy separation that we observe between the two higher energy absorption peaks. This splitting is in good agreement with photoabsorption results obtained in the 5p region on Dy atomic vapour [26] ; it decreases with decreasing atomic number and so becomes probably too small to be clearly distinguished in LaF_3. However, and as already explained, transitions from the valence band to higher energy states in the conduction band contribute to the absorption in the region of 5p excitations and so may partly obscure the spin-orbit doublets ; these valence band excitations may be also responsible for additional absorption structures like the weak shoulder around 23 eV in DyF_3.

The occurrence of strong individual transitions either from the valence band or from the 5p lanthanide subshell between 10 and 40 eV means that over this energy range a sharply defined plasma resonance cannot be associated with a single peak in the electron energy loss spectra ; collective excitations probably spread out over this relatively large energy range.

In metallic dysprosium as in gadolinium, the larger peak around 14 eV in the volume loss spectrum (Fig. 13) involves a volume plasmon excitation whereas the second main loss peak at about 36 eV appears mostly related to the 5p excitations as in DyF_3 ; the maximum on the derived photoabsorption curve (Fig. 15) occurs just a little lower in energy than in the trifluoride, in accordance with a photoemission determination of the O_2 and O_3 level positions [19, 25]. The well marked shoulder on the low energy side of this absorption peak could be accordingly related to the spin-orbit splitting of the initial $5p_{1/2}$-$5p_{3/2}$ states. Our results are in reasonable agreement with previously reported energy loss spectra as far as peak positions are concerned [15, 23]. In addition, the reflectivity curves derived from our data (Figs. 16 and 17) exhibit in Gd and Dy the same general behaviour as the ones determined by direct optical measurements [4]. The high energy part of the loss spectra is quite similar in metallic dysprosium and in its fluoride ; as it involves 4d electron excitations, it will be described below for both materials.

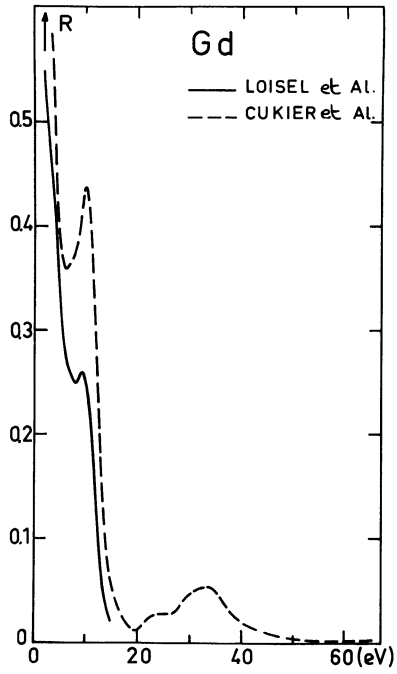

Fig. 16. — Normal reflectance of Gd from our data (———) and from optical measurements (——).

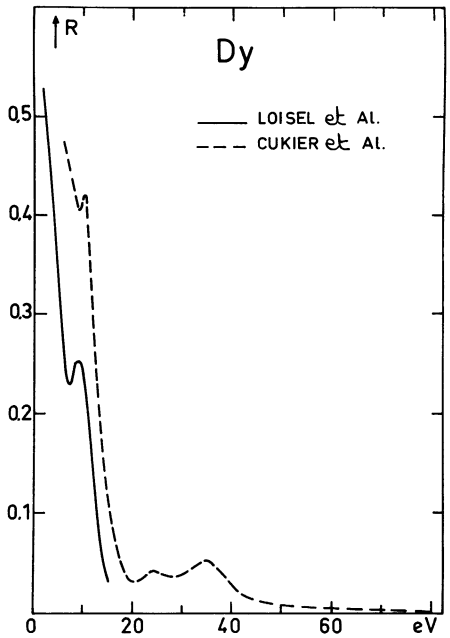

Fig. 17. — Normal reflectance of Dy from our data (———) and from optical measurements (——).

4.2.2 4d *electron excitations.* — The photoabsorption curves and energy loss functions display a nearly similar shape in this energy range ; both curves exhibit a large peak above 100 eV whose position is almost identical in the metal and in its fluoride. A comparison with photoemission [19] and photoabsorption data [1] in metals shows that these strong absorption maxima are due to the excitation of the 4d electrons. We observe a gradual modification of these peaks with increasing atomic number : their maxima move towards higher energies — from about 119 eV in LaF_3 to 148 eV in Gd and 162 eV in Dy — while their intensities become lower as the number of vacancies available in the 4f subshell is decreasing ;

a similar evolution is observed in the first-row transition elements for the 3p electron excitations [8, 12].

Our measurements are in accordance with qualitative data previously obtained on Gd and Dy in the 4d energy range by inelastic scattering of electrons [27]. The large asymmetrical peak observed in LaF_3 (Fig. 18, raw energy loss spectrum) appears to be closely similar to the 4d photoabsorption spectra in lanthanum vapour and solid as reported in [28]; its quasi-resonant behaviour is predicted by atomic calculations [14, 20, 21, 29, 30]. More generally, the strong 4d absorption peak in these lanthanides as in their fluorides results from atomic

$$4d^{10}\,4f^{n} \rightarrow 4d^{9}\,4f^{n+1}$$

transitions in lanthanide ion. The higher energy states of the $4d^9\,4f^{n+1}$ configuration are predominant and decay non-radiatively through various channels, mainly into $4d^9\,4f^n\varepsilon f$ and $4d^{10}\,4f^{n-1}\,\varepsilon l$ as indicated by recent photoemission results [31]; these non-radiative decays would be responsible for the broadening of the multiplet lines.

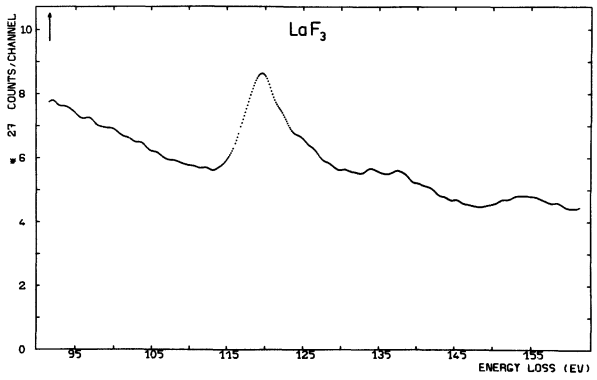

Fig. 18. — Raw energy loss spectrum of LaF_3 in the range of 4d electron excitations.

4.3 URANIUM AND THORIUM FLUORIDES. — The volume loss spectra in uranium and thorium metals have been previously described [32, 33]; they exhibit below 40 eV a broad and prominent band with some superimposed structures. This low energy part of the loss spectra is probably dominated by collective excitations which are however heavily broadened and modulated by strong individual transitions occurring in the same energy range and involving chiefly 6p electrons; the structures in this *collective band* would therefore be like a fingerprint of optical oscillator strength distributions [33].

Above 80 eV, the spectra in both metals as in their fluorides (Figs. 19 and 20) display two large peaks in the range of 5d electron excitations, in satisfactory agreement with direct photoabsorption measurements [34]. In addition, the photoabsorption peaks derived from energy loss data exhibit nearly similar overall shapes and positions in the fluoride as in the metal (Figs. 21 and 22) and so may be inter-

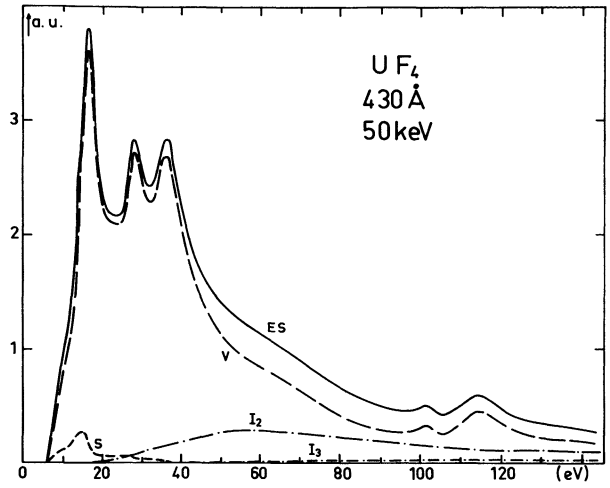

Fig. 19. — Analysis of the experimental energy loss spectrum of UF_4 in its different contributions.

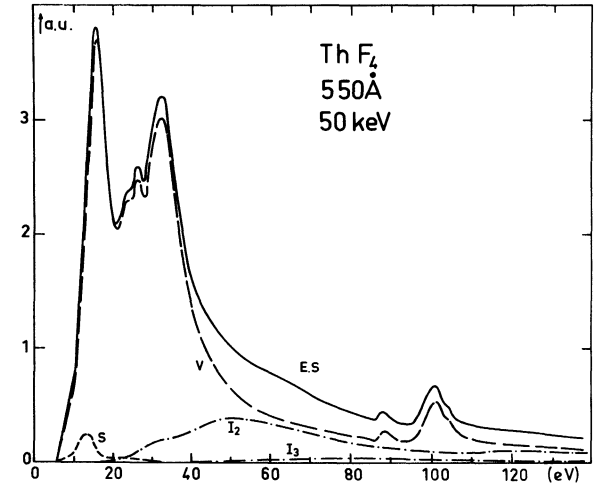

Fig. 20. — Analysis of the experimental energy loss spectrum of ThF_4 in its different contributions.

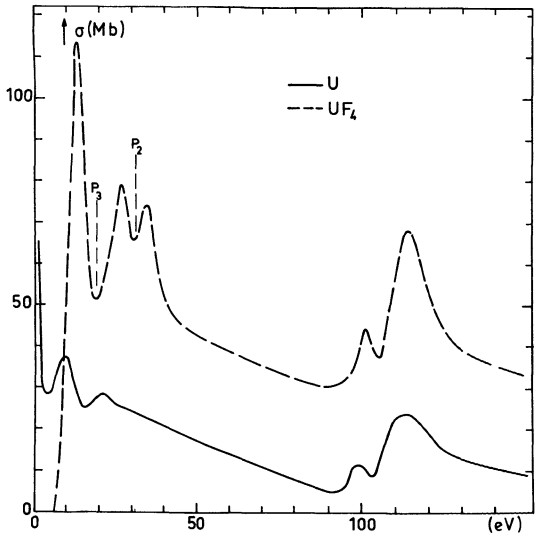

Fig. 21. — Derived photoabsorption cross-section of U and UF_4; the P_2 and P_3 levels are reported from ref. [36].

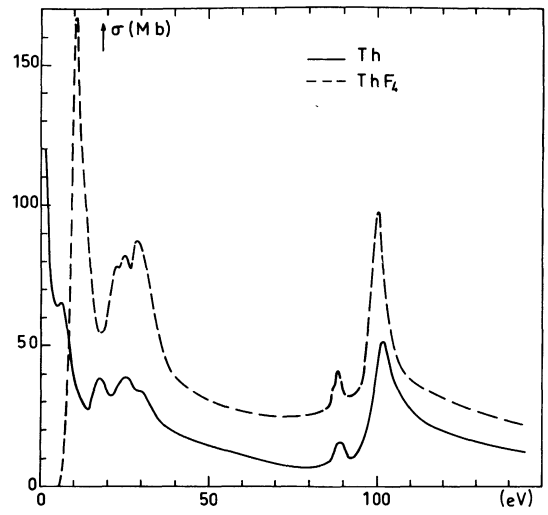

Fig. 22. — Derived photoabsorption cross-section of Th and ThF_4.

preted in these compounds along the lines already discussed for the metals [34]. The positions of these peaks are very close to those observed by photoabsorption [34, 35]. The raw spectrum of ThF_4 (Fig. 23) illustrates the quality and the accuracy of energy loss data, even in this high energy range.

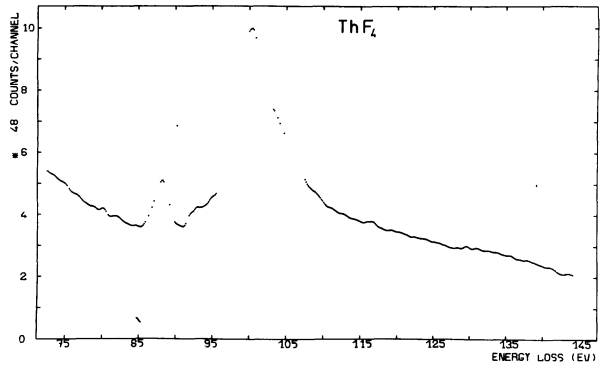

Fig. 23. — Raw energy loss spectrum of ThF_4 in the range of 5d electron excitations.

The following discussion will therefore be restricted to an analysis of the fluoride optical properties in the low energy range.

4.3.1 UF_4. — Below 50 eV, the volume loss spectra (Fig. 19) as well as the derived photoabsorption curve (Fig. 21) appear much more structured in the fluoride than in the metal itself [32] and display three sharp and well separated peaks. However, the heavily absorbing character of metallic uranium samples makes an accurate setting of the spectrometer more difficult to achieve and so reduces the actual energy resolution; this fact is probably partly responsible of a broadening of the loss peaks in uranium spectra.

The derived photoabsorption curve (Fig. 21) rises steeply above 6 eV and reaches a maximum around 13 eV; on account of photoemission data [36], this prominent peak is assigned to transitions originating from F^- 2p levels which give rise to a U-F *bonding band* consisting of fluorine 2p electrons and metal 6d, 7s and 5f electrons. This bonding band appears to be very similar in UO_2 and in UF_4, except for a shift of about 2 eV towards higher binding energies in UF_4, which is consistent with an increase of anion electronegativity when passing from oxygen to fluorine compounds [36].

The second and third absorption peak respectively located around 26 and 34 eV may be mostly attributed to the excitation of uranium 6p electrons by a comparison with the P_2 and P_3 levels energy values recently reported [36]. However this $6p_{3/2}$-$6p_{1/2}$ doublet is probably somewhat disturbed by a contribution from transitions issued from the bonding band and not yet exhausted in this energy range, since $n_{\text{eff}}(\varepsilon_2)$ reaches a value of only 20 towards 40 eV.

4.3.2 ThF_4. — As far as we know, this is the first determination of optical properties of this compound in this energy range. As in UF_4, a quite large and sharp photoabsorption peak located around 11 eV (Fig. 22) involves a low energy part of transitions from the Th-F valence bonding band to the conduction band. The second absorption peak occurring between 20 and 40 eV displays some structures and appears chiefly associated with thorium 6p electron excitations in analogy to the positions of the P_2 and P_3 levels as measured in ThO_2 by X-ray photoelectron studies [37, 38]. However the $6p_{3/2}$-$6p_{1/2}$ doublet is not so clearly separated as in UF_4; in addition to a smaller spin-orbit splitting in ThF_4 as compared to UF_4, this fact may be due to a larger contribution in this absorption range of the higher energy part of the transitions originating from the bonding band. Indeed these transitions are not completely exhausted below about 40 eV as indicated by the $n_{\text{eff}}(\varepsilon_2)$ values (Fig. 24).

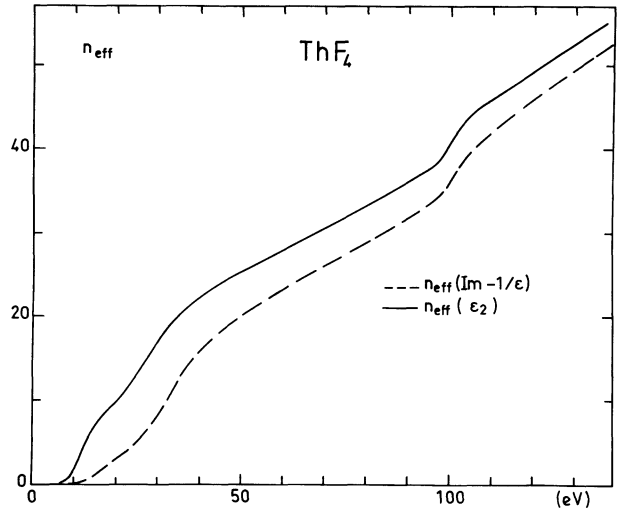

Fig. 24. — Effective number calculated for optical excitations $n_{\text{eff}}(\varepsilon_2)$ and for electron energy losses $n_{\text{eff}}(-\text{Im } 1/\varepsilon)$ of ThF_4.

5. **Summary and conclusions.** — The electron energy loss spectra and the derived photoabsorption cross-sections exhibit between 30 and 60 eV a great similitude in all the materials investigated, metals as well as oxides or fluorides; the predominant excitations in this energy range involve transitions from the p outermost core levels of the metal ion. The corresponding absorption peaks are just shifted a few eV towards higher energies in passing from the pure metal to its compound, oxide or fluoride. In heavy metals Gd, Dy, U, Th and their compounds, we observe in this energy range a double absorption peak probably mostly associated with the $p_{3/2}$-$p_{1/2}$ spin-orbit splitting.

Above 80 eV, the absorption peaks are almost identical and nearly at the same position in lanthanide and actinide metals and in their fluorides; these peaks are attributed to atomic transitions originating from the 4d or 5d subshells of the metal ion.

Below 30 eV, the photoabsorption curve of a pure metal appears on the contrary quite different from that of its compound. In all investigated oxides and fluorides, the strong absorption peak rising just beyond the energy gap is ascribed to interband transitions excited from the filled valence band and arising chiefly from F^- or O^- 2p levels; these individual transitions make it arbitrary to assign a single peak in the energy loss spectra to a sharply defined plasma resonance. By contrast, in metallic Sc, Y, Gd and Dy, the energy loss spectra are dominated in this low energy range by the excitation of collective oscillations of valence electrons. The situation is more complex in uranium and thorium; strong interband transitions occurring at low energies in these actinides are not clearly separated from collective excitations and give rise to an extended *collective band* in the energy loss spectra; this band is more or less modulated by the fingerprint of individual transitions.

Acknowledgments. — The authors wish to thank Dr. P. Maletras and Dr. P. Vigier for the investigation of Sc and Sc_2O_3 samples by electron diffraction and microscopy.

References

[1] ZIMKINA, T. M., FOMICHEV, V. A., GRIBOVSKII, S. A. and ZHUKOVA, I. I., *Sov. Phys. Solid State* **9** (1967) 1128.
[2] HAENSEL, R., RABE, P. and SONNTAG, B., *Solid State Commun.* **8** (1970) 1845.
[3] STEPHAN, G., NISAR, M., ROTH, A., *C. R. Hebd. Séan. Acad. Sci.* **274B** (1972) 807.
[4] LOISEL, B., Thèse de spécialité, Rennes (1978).
[5] OLSON, C. J., PIACENTINI, M., LYNCH, D. W., *Phys. Rev.* **B 18** (1978) 5740.
[6] CARILLON, A. and GAUTHE, B., *Third European Conference on Electron Microscopy*, Prague (1964) and *C. R. Hebd. Séan. Acad. Sci.* **263B** (1966) 1242.
[7] WEHENKEL, C., *J. Physique* **36** (1975) 199.
[8] WEHENKEL, C., GAUTHE, B., *Phys. Status Solidi* (b) **64** (1974) 515.
[9] WEHENKEL, C., Thèse, Paris (1975).
[10] WEHENKEL, C., GAUTHE, B., *Second. Int. Conf. on inner shell ionization phenomena*, Freiburg (1976) 91.
[11] BEARDEN, J. A., BURR, A. F., *Rev. Mod. Phys.* **39** (1967) 125.
[12] SONNTAG, B., HAENSEL, R. and KUNZ, C., *Solid State Commun.* **7** (1969) 597.
[13] COMBET FARNOUX, F., *Physica Fennica* **9** (suppl. 51) (1974) 80.
[14] DEHMER, J. L., STARACE, A. F., FANO, U., SUGAR, J. and COOPER, J. W., *Phys. Rev. Lett.* **26** (1971) 1521.
[15] COLLIEX, C., GASGNIER, M., TREBBIA, P., *J. Physique* **37** (1976) 397.
[16] BROUSSEAU-LAHAYE, B., COLLIEX, C., FRANDON, J., GASGNIER, M. and TREBBIA, P., *Phys. Status Solidi* (b) **69** (1975) 257.
[17] BALABANOVA, L. A., STEPIN, E. V., *Sov. Phys. Solid State* **19** (1977) 1766.
[18] ABRAMOV, V. N., KUZNETSOV, A. I., *Sov. Phys. Solid State* **20** (1978) 399.
[19] DUFOUR, G., Thèse, Paris (1978).
[20] WENDIN, G., *Phys. Lett.* **46A** (1973) 119.
[21] AMUSIA, M. Ya. and SHEFTEL, S. I., *Phys. Lett.* **55A** (1976) 469.
[22] LYNCH, M. J., SWAN, J. B., *Australian J. Phys.* **21** (1968) 811.
[23] DANIELS, J., *Opt. Commun.* **3** (1971) 13.
[24] WEAVER, J. H., OLSON, C. G., *Phys. Rev.* **B 15** (1977) 590.
[25] WERTHEIM, G. K., COHEN, R. L., ROSENCWAIG, A., GUGGENHEIM, J., *International Conference on electron spectroscopy*, Asilomar (1971) VI, 2.
[26] TRACY, D. H., *Proc. R. Soc. London* **A 357** (1977) 485.
[27] TREBBIA, P., COLLIEX, C., *Phys. Status Solidi* (b) **58** (1973) 523.
[28] CONNERADE, J. P., *Contemp. Phys.* **19** (1978) 415.
[29] COMBET FARNOUX, F., *Proc. Int. Conf. on Inner Shell Ionization Phenomena* (Atlanta) 1972 Vol. **2** 1130.
[30] DEHMER, J. L. and STARACE, A. F., *Phys. Rev.* **B 5** (1972) 1792.
[31] LENTH, W., LUTZ, F., BARTH, J., KALKOFFEN, G. and KUNZ, C., *Phys. Rev. Lett.* **41** (1978) 1185.
[32] WEHENKEL, C. and GAUTHE, B., *Opt. Commun.* **11** (1974) 64.
[33] WEHENKEL, C., GAUTHE, B. and CUKIER, M., *5th Int. Conf. on Vacuum Ultraviolet Radiation Physics*, Montpellier (1977), I, 10.
[34] CUKIER, M., DHEZ, P., GAUTHE, B., JAEGLE, P., WEHENKEL, C. and COMBET FARNOUX, F., *J. Physique Lett.* **39** (1978) L-315.
[35] LIAKHOVSKAIA, I. I., IPATOV, V. N., ZIMKINA, T. M., *J. Strouktournoi Chimii* **18** (1977) 668.
[36] PIREAUX, J. J., MARTENSSON, R., DIDRIKSSON, R., SIEGBAHN, K., RIGA, J. and VERBIST, J., *Chem. Phys. Lett.* **46** (1977) 215.
[37] VEAL, B. W. and LAM, D. J., *Phys. Rev.* **B 10** (1974) 4902.
[38] FUGGLE, J. C., BURR, A. F., WATSON, L. M., FABIAN, D. J. and LANG, W., *J. Phys. F. : Metal Phys.* **4** (1974) 335.